

## The power of branched chains: optimising functional molecular materials

Cite this: DOI: 10.1039/c3tc31381f

Martin J. Hollamby<sup>a</sup> and Takashi Nakanishi<sup>\*b</sup>

The power of branched alkyl substituents to alter material properties is known to soft matter chemistry, with examples found in both surfactants and ionic liquids. Here, we highlight their potency in organic molecular/polymeric materials with optoelectronic applications. Attaching branched alkyl chains to the active  $\pi$ -conjugated core modulates core–core interactions and thus softens the material. This can lead to optimised assemblies with improved optoelectronic properties. By increasing the number and volume of the flexible chains, individual cores can be isolated, yielding functional organic liquids with bulk optical properties the same as the intrinsic molecular characteristics obtained for their dilute solutions. These liquid materials can accommodate dopants to offer diverse and tuneable emission colours, and provide an easily applicable flexible and foldable continuous layer for future optoelectronic media.

Received 17th July 2013  
Accepted 22nd August 2013

DOI: 10.1039/c3tc31381f

[www.rsc.org/MaterialsC](http://www.rsc.org/MaterialsC)

### 1. Introduction

Optoelectronically-active  $\pi$ -conjugated organic molecules or polymers tend to be highly crystalline and have low solubility in most common solvents. Consequently, they are unsuitable for application in flexible devices and cannot easily be processed by inexpensive and convenient solution-state methods. To soften the bulk material and to facilitate solution processing, solubilising groups are commonly covalently attached to these

<sup>a</sup>School of Physical and Geographical Sciences, Keele University, Keele, Staffordshire, ST55BG, UK. E-mail: [m.hollamby@keele.ac.uk](mailto:m.hollamby@keele.ac.uk); Fax: +44 1782 712378; Tel: +44 1782 733532

<sup>b</sup>National Institute for Materials Science (NIMS), 1-2-1 Sengen, Tsukuba 305-0047, Japan. E-mail: [NAKANISHI.Takashi@nims.go.jp](mailto:NAKANISHI.Takashi@nims.go.jp); Fax: +81 29 859 2101; Tel: +81 29 860 4740



Martin Hollamby is a lecturer at Keele University, UK and has held this position since at the end of May 2013. He received a PhD at the University of Bristol, UK where he worked in the group of Professor J. Eastoe on topics within surfactant chemistry. In 2009 he moved to the Max-Planck Institute of Colloids and Interfaces, Potsdam-Golm, Germany, where he worked with Prof. H. Moehwald on corrosion-

resistant coatings. In 2011 Martin was awarded a JSPS post-doctoral fellowship to work in NIMS (National Institute for Materials Science, Tsukuba, Japan) with Dr T. Nakanishi and subsequently obtained a position as an independent researcher in the International Center for Young Scientists at NIMS, where he remained until May 2013. His research focuses on molecular self-assembly for organic electronics, and the application of scattering techniques, including SANS, for characterizing the structure and formation mechanisms of condensed matter.



Takashi Nakanishi is currently a Principal Researcher at the National Institute for Materials Science (NIMS) in Japan. He completed the doctoral course in shorter period at Nagasaki University, Japan, in 2000. After JSPS post doctoral researches at Houston University, USA, and at Oxford University, UK, he joined NIMS in 2004. Since 2010, he has been in his current position. In 2007-2010, he was also a

group leader at the Max Planck Institute of Colloids and Interfaces, Germany, and in 2007-2011, he was a researcher of PRESTO, Japan Science and Technology Agency. Since 2011 he is being also a visiting Professor at Warsaw University of Technology, Poland. His research interest is the development of self-assembly controlled functional soft materials including dimension and morphology regulated molecular materials as well as functional organic molecular liquids.

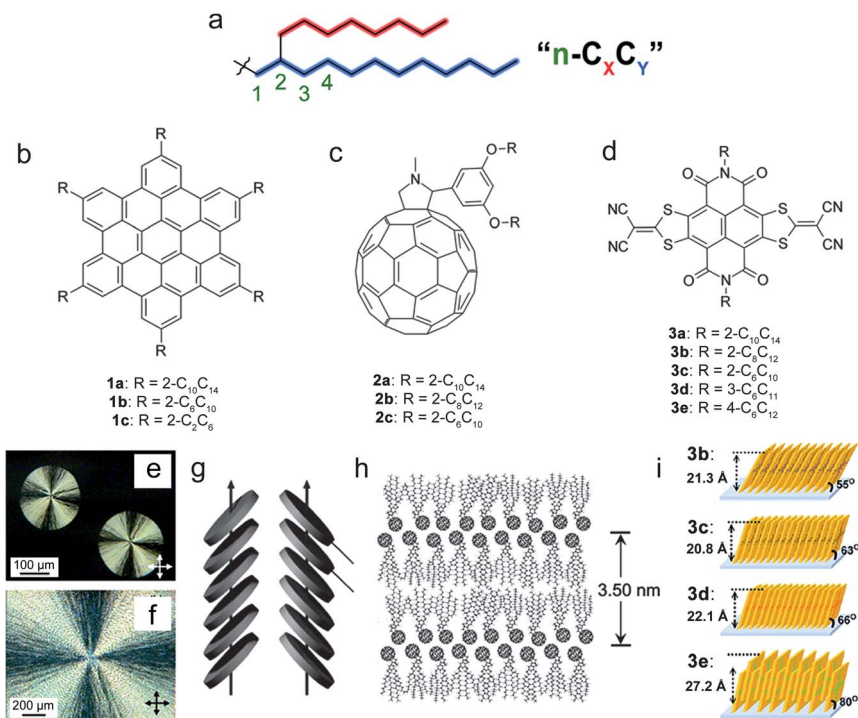


**Fig. 1** (a) General structure of most of the branched chains discussed in this Highlight. (b) Structure of HBC derivatives **1a–c**.<sup>8</sup> (c) Structure of C<sub>60</sub> derivatives **2a–c**.<sup>10</sup> (d) Structure of extended-core NDI derivatives **3a–e**.<sup>18,19</sup> (e and f) Polarising optical microscope images of spherulites of **1a** crystallised at (e) 35 °C and (f) 38 °C. Reprinted with permission from ref. 6. Copyright 2004 American Chemical Society. (g) The herringbone structure found for assemblies of **1a–c** at room temperature. Reprinted with permission from ref. 8. Copyright 2006 American Chemical Society. (h) Molecular packing in the room-temperature smectic liquid crystalline phase formed by **2b**. Reproduced from ref. 10 with permission from The Royal Society of Chemistry. (i) The different film structures formed by derivatives **3b–e** after thermal treatment. Reprinted with permission from ref. 19. Copyright 2013 American Chemical Society.

$\pi$ -conjugated moieties. Historically, linear *n*-alkyl chains have been used. However, the use of branched alkyl substituents has recently become more widespread. Branched alkanes typically have quite different properties (*e.g.* melting point, viscosity, density, surface tension) from their linear counterparts. Generally, this derives from their higher chemical stability and bulk, but lower cohesivity. As such, attaching branched alkyl chains tends to soften the  $\pi$ -conjugated material to a greater extent than attaching linear *n*-alkyl chains.

The ability of branched chains to tune both the molecular-scale and bulk material properties of soft matter is already known. For example, incorporating branched chains into ionic liquids<sup>1</sup> can influence various properties, including the decomposition and glassy transition temperatures (higher in both cases for a Cl<sup>−</sup> counterion). In another example, hydrocarbon surfactants with branched and highly methylated chains were found to perform efficiently in liquid CO<sub>2</sub>, forming micelles and stabilising water droplets.<sup>2</sup> This was significant because previously only fluorocarbon surfactants and polymers had been found to exhibit such behavior.<sup>3</sup> The high efficiency conveyed by branched alkyl substituents is thought to be due to their low interfacial free volume<sup>4</sup> and high surface coverage.<sup>5</sup>

Here, we highlight the advanced control afforded by branched alkyl substituents (*e.g.* Fig. 1a) in systems with applications in organic optoelectronics. This is discussed for both small conjugated molecules and polymers. As detailed in the following sections, branched substituents can significantly

soften the material. This not only facilitates solution processing, but also permits the growth of larger assemblies with improved bulk properties or new functional organic liquids.

## 2. Controlling self-assembly

### 2.1. Molecular assemblies

In a series of studies on the organisational behaviour of hexa-*peri*-hexabenzocoronene (HBC)<sup>6–8</sup> and other related polycyclic aromatic molecules,<sup>9</sup> Müllen *et al.* have clearly outlined the possibilities afforded by the use of branched chains. Symmetrically functionalising HBC with six 2-decyltetradecyl (2-C<sub>10</sub>C<sub>14</sub>) chains (**1a**, Fig. 1b) was found to lower the isotropization temperature to 46 °C.<sup>6</sup> This was a substantial reduction in comparison to *n*-alkyl substituted HBCs (>400 °C). Spherulites with extremely long-range internal order (*e.g.* Fig. 1e and f) were obtained. Shortening the chains (**1a–c**) led to assemblies with higher isotropization temperatures.<sup>7</sup> Bulkier side chains were thought to better modulate the assembly process by reducing the strong core–core interactions, lowering the nucleation rate of the discotic assembly and thereby permitting larger structures to grow.<sup>5</sup> All of the molecules formed ordered herringbone structures (Fig. 1g) with high charge carrier mobilities and long charge carrier lifetimes.<sup>8</sup> The length and flexibility of the alkyl chains was also thought to disfavour contact with polar substrates (*e.g.* glass or indium tin oxide). This favours edge-on packing and increases the speed of charge transport.

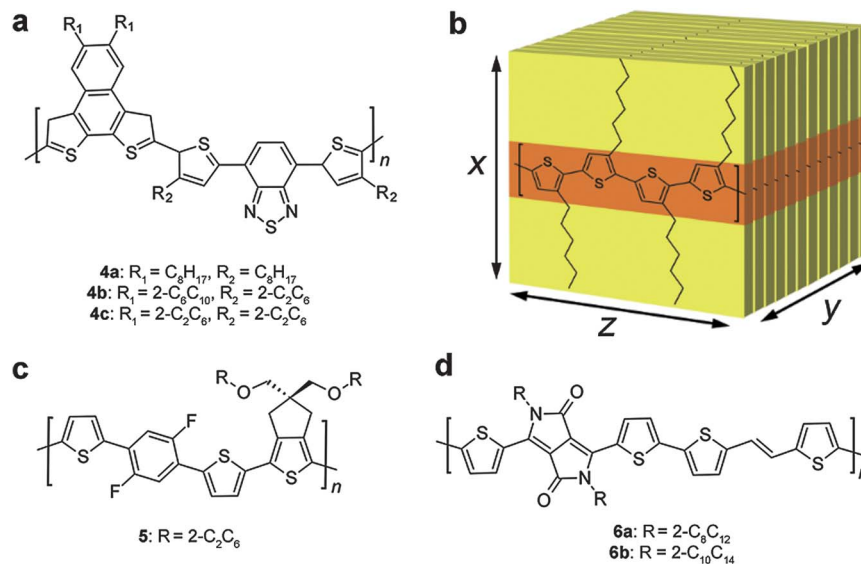


**Fig. 2** (a) Structure of  $\pi$ -conjugated polymer **4**,<sup>22</sup> containing alternating naphtho[2,1-*b*:3,4-*b'*]dithiophene and 4,7-di(thiophen-2-yl)benzothiadiazole units, which was used to compare various alkyl substituent structures and positions, e.g. **4a–c**. (b) Schematic representation of the layered assembly structure formed by many conjugated polymers in the film state. (c) Structure of  $\pi$ -conjugated polymer **5**.<sup>28</sup> (d) Structure of  $\pi$ -conjugated polymer **6**, containing diketopyrrolopyrrole units.<sup>26</sup>

Charge carrier mobility is affected by molecular orientation, which can also be influenced by the chemistry of the attached side chains. Within a discotic column, a confirmation of HBC cores with a twisting angle of either  $0^\circ$ ,  $60^\circ$  or  $120^\circ$  was expected to provide the highest mobility by maximising overlap.<sup>9</sup> By changing the structure of the side chains, phases containing predominantly a  $60^\circ$  twist were prepared. The highest mobility values, of around  $0.2 \text{ cm}^2 \text{ V}^{-1} \text{ s}^{-1}$ , were indeed noted in these phases.<sup>9</sup> However, even in these controlled cases, structural defects were present that significantly impacted on the measured carrier mobility. It remains an open challenge to remove such defects to meet the predicted high performances.

Building on that pioneering work, our group has studied the effect of changing the type, number and substituent position of various branched chains on the self-assembly properties of  $C_{60}$ .<sup>10,11</sup> Some of the investigated  $C_{60}$  derivatives are shown in Fig. 1c (**2a–c**). This followed previous work in which linear chains were investigated.<sup>12</sup> In both cases, a variety of crystalline,<sup>13</sup> liquid crystalline<sup>14</sup> and even liquid<sup>11,15,16</sup> (e.g. **2a**) materials have been reported. However, the use of branched chains significantly softens the materials, lowering the glassy transition temperature ( $T_g$ ) and permitting greater control over assembly properties.<sup>10</sup> For the molecules exhibiting liquid crystalline phases (**2b,c**), both the isotropization and crystallization temperatures were decreased, in similarity to the results seen for the HBC derivatives.<sup>6–8,17</sup> In particular, **2b** possessed a smectic liquid crystalline phase (Fig. 1h) extending from  $84^\circ \text{C}$  to below room temperature. The performance of organic photovoltaic devices containing **2b** alongside poly(3-hexylthiophene) (P3HT) was found to be comparable to conventional phenyl- $C_{61}$ -butyric acid methyl ester (PCBM)/P3HT bulk heterojunction solar cells tested in the same way. This signified that  $C_{60}$  derivatives bearing branched chains have the potential to act as electron acceptors in flexible photovoltaic devices.

Elsewhere, the influence of both the length and position of the branching point of chains attached to extended core naphthalene diimides (NDIs) was investigated.<sup>18,19</sup> While studies have primarily focussed on obtaining high electron mobilities, attempts have been made to correlate these properties with the assembly structures. Initially, **3a**† and **3b** were compared.<sup>18</sup> The film of **3b** had higher electron mobility after annealing, although a reason for this was not given. By moving the branching point, looking at derivatives **3b–e**, mobility values ranging from less than 0.2 to over  $3.0 \text{ cm}^2 \text{ V}^{-1} \text{ s}^{-1}$  were reported, that additionally depended on device geometry. The varied performance was explained by the difference in orientation and packing within the layered film (Fig. 1i). In this case, **3d** yielded the most desirable packing, being the most edge-on to the substrate and permitting the greatest overlap between NDI cores.<sup>19</sup>

## 2.2. Polymer assemblies

Several studies have recently probed the influence of alkyl side-chain structure and position on the properties of conjugated polymer-based optoelectronic devices. It was noted that the side-chain chemistry, in addition to controlling factors such as solubility and therefore ease of processing, can strongly influence the electronic properties of the polymer film. In particular, replacing linear with branched chains typically lowers the HOMO level of the polymer.<sup>20–22</sup> For example, for **4a** (Fig. 2a, linear side-chains), HOMO =  $-5.13 \text{ eV}$ , whereas for **4b**, HOMO =  $-5.33 \text{ eV}$  and **4c**, HOMO =  $-5.34 \text{ eV}$  (Fig. 2a, branched side-chains).<sup>22</sup> This reduction can have a large influence on parameters such as open-circuit voltage,  $V_{OC}$  and short circuit current

† This is incorrectly described in the original paper as having “2-decyltetraicosyl” chains.

density,  $J_{SC}$  of solar cell devices.<sup>20–22</sup> By controlling the branched side-chain chemistry, these values can be optimised for each polymer–fullerene combination and a high efficiency obtained.<sup>23</sup>

Conjugated polymers typically form layered assemblies (Fig. 2b) in the film state.<sup>24</sup> Several studies have looked at the effect on film structure of replacing linear alkyl side-chains with branched ones. While multiple factors, including the rigidity and strength of interactions between neighbouring backbones must be considered where comparing trends, the use of bulkier chains with a larger carbon number (e.g. **4b** vs. **4a**, **4c**)<sup>22</sup> tends to increase the interlayer spacing  $d_{100}$  ( $x$  direction, Fig. 2).<sup>25,26</sup> Increasing the attachment density of chains has the same effect.<sup>27,28</sup> The increase in  $d_{100}$  has recently been ascribed to a reduced interdigitation between the side-chains of **5** (Fig. 2c), which led to better alignment within each layer.<sup>28</sup> However,  $d_{100}$  was found to decrease when branched side-chains with the same or similar number of carbon atoms as their linear counterparts (e.g. **4c** vs. **4a**) were used.<sup>20–22</sup>

The effect of using branched chains on the  $\pi$ – $\pi$  distance,  $d_{010}$  ( $y$  direction, Fig. 2b), which is thought to be an important factor for fast charge transport, seems to be more polymer-specific. In some cases,  $d_{010}$  increased when bulkier side chains were used, leading to poorer solar cell performance.<sup>22</sup> However, increasing the bulk of the side-chains by using longer chains (e.g. **6a** and **6b**, Fig. 2d), or by moving the branching point away from the polymer backbone decreased  $d_{010}$ .<sup>25,26</sup>

In these latter studies a correlation between closer  $\pi$ – $\pi$  overlap and higher carrier mobility was drawn. However, it was

recognised that to obtain the best charge carrier mobilities (up to  $8.2 \text{ cm}^2 \text{ V}^{-1} \text{ s}^{-1}$  for **6b**), other factors such as polymer conformation and orientation had to be taken into account.

In such assemblies, an edge-on geometry (*i.e.* with the substrate in the  $xz$  plane of Fig. 2b) is desirable as it permits two fast transport directions through the polymer itself ( $z$  direction) and through  $\pi$ – $\pi$  interactions ( $y$  direction) between overlapping polymers.<sup>24</sup> Branched chains have been found to influence this orientation. In particular, a higher attachment density led to a greater proportion of face-on oriented backbones, even after annealing.<sup>27</sup> Elsewhere, the greater bulkiness of branched side-chains was thought to decouple the conjugated backbone from dipoles within the substrate, thereby reducing the effect of gate dielectric on the charge carrier mobility.<sup>29</sup>

In summary, the use of branched side-chains has a similar effect in both molecular and polymer assemblies. The materials are softened, *via* greater modulation of the  $\pi$ -stacking interactions between the cores. The bulkiness of the chains influences molecular orientation and packing. It is therefore clear that the molecular orientation, packing and crystallinity can be optimised by controlling the length, position and structure of the branched groups. This in turn can be used to generate enhanced optoelectronic device layers. However, general methods to control the assembly structure are still lacking. Additionally, in most cases the structures expected to provide the best optoelectronic properties have yet to be identified. Addressing this may require a mainstream shift away from studies focussing primarily on optoelectronic device properties, which are strongly dependent on factors other than the assembly, to those

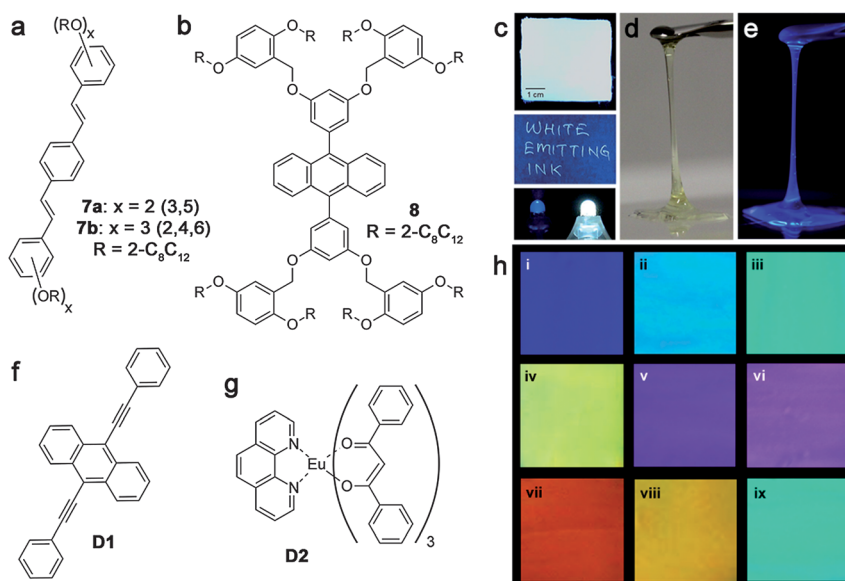


**Fig. 3** (a) Structure of oligo(*p*-phenylene-vinylene) derivatives **7a,b**.<sup>32</sup> (b) Structure of anthracene derivative **8**.<sup>33</sup> (c) Various images of a **7b** based composite painted or written with a ballpoint pen onto substrates, and pasted onto a commercially available UV-LED (left: before application, right: after). Reprinted with permission from ref. 32. Copyright 2012 Wiley-VCH. (d and e) Photos of liquid anthracene derivative **8** under (d) normal and (e) UV light ( $\lambda_{ex} = 365 \text{ nm}$ ). Reprinted from ref. 33, under a Creative Commons Attribution 3.0 Unported (CC BY) license. (f) Structure of dopant **D1**, 9,10-bis(phenylethynyl)anthracene.<sup>33</sup> (g) Structure of dopant **D2**, tris(1,3-diphenyl-1,3-propanedionato)(1,10-phenanthroline)europium(III).<sup>33</sup> (h) Example of the scope of emission colour tuning afforded by blending **8** with **D1** and **D2** as follows: (i) **8** alone, (ii) **8** + **D1** at 0.3 mol%, (iii) **8** + **D1** at 0.5 mol%, (iv) **8** + **D1** at 2.0 mol%, (v) **8** + **D2** at 2.0 mol%, (vi) **8** + **D2** at 5.0 mol%, (vii) **8** + **D1** at 0.5 mol% + **D2** at 5.0 mol%, 20 °C, (viii) **8** + **D1** at 0.5 mol% + **D2** at 5.0 mol%, 50 °C, (ix) **8** + **D1** at 0.5 mol% + **D2** at 5.0 mol%, 100 °C. Adapted from ref. 33, under a Creative Commons Attribution 3.0 Unported (CC BY) license.



## Highlight

focussing on layer structure. By pinpointing optimum structures and general methods to achieve them, a pathway towards the next generation of molecular optoelectronic materials may more easily be identified.

### 3. Functional liquids

Attaching branched chains to  $\pi$ -conjugated molecules can provoke a liquid state at room temperature (e.g.  $C_{60}$  derivative **2a**).<sup>10</sup> This is partly due to the natural reduction in solidification/glassy transition temperature afforded by the addition of bulky, flexible groups. However, it is also due to the consequential disruption of the  $\pi$ - $\pi$  interactions between  $\pi$ -conjugated cores. These non-volatile functional organic liquids can be desirable for flexible/foldable devices for their ease of application and ability to form a continuous layer. Because they can flow, electrodes and the functional active layer will remain connected even after significant bending. Additionally, the liquids can accommodate small dopant molecules. The first functional organic liquid to be used in an optoelectronic device was recently reported.<sup>30</sup> A liquid carbazole derivative with a 2-ethylhexyl ( $2-C_2C_6$ ) chain was obtained with a hole mobility of  $4 \times 10^{-6} \text{ cm}^2 \text{ V}^{-1} \text{ s}^{-1}$ . This was used as part of the active layer in an organic light emitting diode with rubrene (5,6,11,12-tetra-phenylnaphthacene). The liquid layer was able to transport charge to rubrene, allowing electroluminescence with a quantum efficiency of around 0.03%. That value was recently improved to 0.3% by the addition of electrolyte.<sup>31</sup> However, both efficiencies remain low for practical use and further improvements are still needed.

In our group, rather different functional organic liquids are being developed (Fig. 3).<sup>32,33</sup> Rather than tuning the assembly properties through modulated core-core interactions, this new approach aims to completely isolate the  $\pi$ -conjugated cores from contact with one another and thereby emphasize the luminescence features of the molecule. In doing this, intrinsic dilute solution-state molecular properties such as absorption and fluorescence are retained in the bulk solvent-free liquid state. The concept is related to that of liquid proteins, in which the protein functionality is kept despite being a bulk liquid.<sup>34</sup>

Two families of liquid derivatives have been reported, based on oligo(*p*-phenylene-vinylene)<sup>32</sup> **7** and anthracene **8** (Fig. 3a and b).<sup>33</sup> In both cases, to find how best to inhibit  $\pi$ - $\pi$  interactions between cores, various alkyl chain structures were compared, including heavily methylated "hyperbranched" chains. A selection of the structures that were studied is given in Fig. 3. **7** and **8**, which possess 2-octyldodecyl ( $2-C_8C_{12}$ ) chains, are all liquids at room temperature. Increasing the number of chains, *i.e.* going from **7a** to **7b**, resulted in a lower complex viscosity, as did the use of  $2-C_8C_{12}$  groups rather than hyperbranched chains. For all of the liquids, the absorption and emission spectra were found to be similar in the bulk liquid state and in dilute solution, with only a small drop in the fluorescence quantum yield ( $\Phi_{\text{FL}} > 55\%$ ). This indicates substantial core isolation. In the case of **8**, the isolation strongly increased the photostability of the anthracene center to UV light-induced oxidation in both the solution and film states. Non-volatile, solvent-free liquids **7** and

**8** are all blue emitting (e.g. Fig. 3e) and could incorporate dopants capable of affecting their emission properties by simply blending with a spatula. In the case of **7**, orange-emitting rubrene and green-emitting tris(8-hydroxyquinolino) aluminium (Alq3) were added. These composites retained their liquid properties and could be applied to various surfaces using a paint brush or a ball-point pen, including a UV-LED (e.g. Fig. 3c).<sup>32</sup> Significantly, they exhibited tuneable white-light emission at a  $\Phi_{\text{FL}}$  of around 35% (Fig. 3c).

Doping **8** with **D1** (Fig. 3f) again yielded a liquid composite.<sup>33</sup> Interestingly, the energy transfer from **8** to **D1** was found to be very efficient (96%) with only a small amount (0.3 mol%) of dopant, which led to a cyan emission colour (Fig. 3h(ii)). Increasing the doping level, up to 5 mol% changed the colour to green and finally yellow (e.g. Fig. 3h(iii) and (iv)), which was probably due to clustering of **D1** in the film. Furthermore, blending **8** with **D2** (Fig. 3g) alone and together with **D1** led to purple and red emission colours at room temperature (e.g. Fig. 3h(v-vii)).<sup>33</sup> **D2** has a thermoresponsive emission, so heating a film containing **8** blended with 0.5 mol% **D1** and 5.0 mol% **D2**, further influenced the emission colour from red (20 °C) to yellow (50 °C) to emerald green (100 °C) (Fig. 3h(vii-ix)).

Doping combinations of various dyes into these emissive fluids is therefore a powerful way to obtain easily manipulated, flexible and stable liquid composite materials with a large degree of control over their emission colour. Of particular advantage is the ability to produce the full palette of colours without needing to synthesise many different dyes. While core isolation may limit the electronic properties of these materials, they clearly represent effective matrices. Through the addition of dopants including conducting polymers or other functional molecules, it is predicted that optoelectronic activity will be strongly enhanced. In this way, particularly flexible and foldable composite layers based on functional organic liquids can be anticipated.

### 4. Conclusions

Branched chains increase the solubility of the  $\pi$ -conjugated molecules while softening the bulk material, allowing for the formation of flexible layers suitable for next-generation wearable devices, without the anticipated loss of performance. Conversely, the material softening can actually permit longer-range order and larger grain sizes than are accessible using linear substituents. This is achieved through greater modulation of the  $\pi$ -stacking interactions between the cores, which reduces the nucleation rate of ordered assemblies and permits more extensive growth. In other cases, liquids can be formed, in which core-core interactions are significantly impeded, permitting intrinsic molecular properties, such as fluorescence, to be preserved in the bulk fluid. Both of these situations rely on the flexibility and steric bulk of the branched alkyl groups. It is therefore clear that using branched chains offers greater tuning of molecular properties, as well as providing new liquid materials that were otherwise unobtainable. Given this, recent reports of liquid crystalline materials with high electron mobilities that consist of a perylene tetracarboxylic bisimide core substituted with branched siloxane

chains are of interest.<sup>35</sup> In comparison to alkyl chains, siloxanes are more flexible, typically further increasing solubility and softening assembly properties, therefore offering more possibilities for structural control.

## Acknowledgements

The work was partially supported by the KAKENHI (23685033, 25620069 and 25104011) from the MEXT, Japan and Nagase Science and Technology Foundation.

## Notes and references

- 1 T. Erdmenger, J. Vitz, F. Wiesbrock and U. S. Schubert, *J. Mater. Chem.*, 2008, **18**, 5267–5273.
- 2 M. J. Hollamby, K. J. Trickett, A. Mohamed, S. Cummings, R. F. Tabor, O. Myakonkaya, S. Gold, S. Rogers, R. K. Heenan and J. Eastoe, *Angew. Chem., Int. Ed.*, 2009, **48**, 4993–4995.
- 3 J. Eastoe, S. Gold and D. C. Steytler, *Langmuir*, 2006, **22**, 9832–9842.
- 4 M. T. Stone, P. G. Smith, S. R. P. da Rocha, P. J. Rossky and K. P. Johnston, *J. Phys. Chem. B*, 2004, **108**, 1962–1966.
- 5 A. Mohamed, M. Sagisaka, M. Hollamby, S. E. Rogers, R. K. Heenan, R. Dyer and J. Eastoe, *Langmuir*, 2012, **28**, 6299–6306.
- 6 W. Pisula, M. Kastler, D. Wasserfallen, T. Pakula and K. Müllen, *J. Am. Chem. Soc.*, 2004, **126**, 8074–8075.
- 7 M. Kastler, W. Pisula, D. Wasserfallen, T. Pakula and K. Müllen, *J. Am. Chem. Soc.*, 2005, **127**, 4286–4296.
- 8 W. Pisula, M. Kastler, D. Wasserfallen, M. Mondeshki, J. Piris, I. Schnell and K. Müllen, *Chem. Mater.*, 2006, **18**, 3634–3640.
- 9 X. Feng, V. Marcon, W. Pisula, M. R. Hansen, J. Kirkpatrick, F. Grozema, D. Andrienko, K. Kremer and K. Müllen, *Nat. Mater.*, 2009, **8**, 421–426.
- 10 H. Li, S. S. Babu, S. T. Turner, D. Neher, M. J. Hollamby, T. Seki, S. Yagai, Y. Deguchi, H. Möhwald and T. Nakanishi, *J. Mater. Chem. C*, 2013, **1**, 1943–1951.
- 11 H. Li, J. Choi and T. Nakanishi, *Langmuir*, 2013, **29**, 5394–5406.
- 12 T. Nakanishi, *Chem. Commun.*, 2010, **46**, 3425–3436.
- 13 T. Nakanishi, Y. Shen, J. Wang, H. Li, P. Fernandes, K. Yoshida, S. Yagai, M. Takeuchi, K. Ariga, D. G. Kurth and H. Möhwald, *J. Mater. Chem.*, 2010, **20**, 1253–1260.
- 14 T. Nakanishi, Y. Shen, J. Wang, S. Yagai, M. Funahashi, T. Kato, P. Fernandes, H. Möhwald and D. G. Kurth, *J. Am. Chem. Soc.*, 2008, **130**, 9236–9237.
- 15 T. Michinobu, T. Nakanishi, J. P. Hill, M. Funahashi and K. Ariga, *J. Am. Chem. Soc.*, 2006, **128**, 10384–10385.
- 16 T. Michinobu, K. Okoshi, Y. Murakami, K. Shigehara, K. Ariga and T. Nakanishi, *Langmuir*, 2013, **29**, 5337–5344.
- 17 W. Pisula, Ž. Tomović, C. Simpson, M. Kastler, T. Pakula and K. Müllen, *Chem. Mater.*, 2005, **17**, 4296–4303.
- 18 X. Gao, C. Di, Y. Hu, X. Yang, H. Fan, F. Zhang, Y. Liu, H. Li and D. Zhu, *J. Am. Chem. Soc.*, 2010, **132**, 3697–3699.
- 19 F. Zhang, Y. Hu, T. Schuettfort, C. Di, X. Gao, C. R. McNeill, L. Thomsen, S. C. B. Mannsfeld, W. Yuan, H. Sirringhaus and D. Zhu, *J. Am. Chem. Soc.*, 2013, **135**, 2338–2349.
- 20 B. Burkhart, P. P. Khlyabich and B. C. Thompson, *Macromolecules*, 2012, **45**, 3740–3748.
- 21 C. Cui, Y. Sun, Z.-G. Zhang, M. Zhang, J. Zhang and Y. Li, *Macromol. Chem. Phys.*, 2012, **213**, 2267–2274.
- 22 L. Yang, H. Zhou and W. You, *J. Phys. Chem. C*, 2010, **114**, 16793–16800.
- 23 R. L. Uy, S. C. Price and W. You, *Macromol. Rapid Commun.*, 2012, **33**, 1162–1177.
- 24 H. Sirringhaus, P. J. Brown, R. H. Friend, M. M. Nielsen, K. Bechgaard, B. M. W. Langeveld-Voss, A. J. H. Spiering, R. a. J. Janssen, E. W. Meijer, P. Herwig and D. M. de Leeuw, *Nature*, 1999, **401**, 685–688.
- 25 T. Lei, J.-H. Dou and J. Pei, *Adv. Mater.*, 2012, **24**, 6457–6461.
- 26 H. Chen, Y. Guo, G. Yu, Y. Zhao, J. Zhang, D. Gao, H. Liu and Y. Liu, *Adv. Mater.*, 2012, **24**, 4618–4622.
- 27 X. Zhang, L. J. Richter, D. M. DeLongchamp, R. J. Kline, M. R. Hammond, I. McCulloch, M. Heeney, R. S. Ashraf, J. N. Smith, T. D. Anthopoulos, B. Schroeder, Y. H. Geerts, D. A. Fischer and M. F. Toney, *J. Am. Chem. Soc.*, 2011, **133**, 15073–15084.
- 28 B.-G. Kim, E. J. Jeong, J. W. Chung, S. Seo, B. Koo and J. Kim, *Nat. Mater.*, 2013, **12**, 659–664.
- 29 H. Yan, Z. Chen, Y. Zheng, C. Newman, J. R. Quinn, F. Dötz, M. Kastler and A. Facchetti, *Nature*, 2009, **457**, 679–686.
- 30 D. Xu and C. Adachi, *Appl. Phys. Lett.*, 2009, **95**, 053304.
- 31 S. Hirata, K. Kubota, H. H. Jung, O. Hirata, K. Goushi, M. Yahiro and C. Adachi, *Adv. Mater.*, 2011, **23**, 889–893.
- 32 S. S. Babu, J. Aimi, H. Ozawa, N. Shirahata, A. Saeki, S. Seki, A. Ajayaghosh, H. Möhwald and T. Nakanishi, *Angew. Chem., Int. Ed.*, 2012, **51**, 3391–3395.
- 33 S. S. Babu, M. J. Hollamby, J. Aimi, H. Ozawa, A. Saeki, S. Seki, K. Kobayashi, K. Hagiwara, M. Yoshizawa, H. Möhwald and T. Nakanishi, *Nat. Commun.*, 2013, **4**, 1969.
- 34 A. W. Perriman, A. P. S. Brogan, H. Cölfen, N. Tsoureas, G. R. Owen and S. Mann, *Nat. Chem.*, 2010, **2**, 622–626.
- 35 M. Funahashi and A. Sonoda, *J. Mater. Chem.*, 2012, **22**, 25190–25197.